

The anatomy of human substantia nigra based on in vivo and post mortem magnetic resonance data and susceptibility mapping

A. I. Blazejewska¹, S. Wharton¹, A. Pitoit², A. Kempf¹, S. Schwarz³, J. Lowe⁴, D. P. Auer³, R. Bowtell¹, and P. A. Gowland¹

¹Sir Peter Mansfield Magnetic Resonance Centre, University of Nottingham, Nottingham, United Kingdom, ²School of Psychology, University of Nottingham, ³Division of Academic Radiology, University of Nottingham, ⁴Division of Pathology, Nottingham University Hospitals NHS Trust

Introduction The substantia nigra (SN), a part of the basal ganglia nuclei, plays an important role in neurodegenerative diseases such as Parkinson's, but the relationship between its anatomy and its appearance on MRI remains unclear. Due to the high iron concentration the SN appears blue in Perl's stained sections images and as a dark structure in T2*-weighted MR images. On the microscopic level the SN can be divided into the pars compacta (SNpc) and pars reticulata (SNpr) based on analysis of the dominant neuron types. Distinct subgroups of dopamine-containing neurons named *nigrosomes* were shown to occur in the SNpc in a histology study using immunostaining for calbindin D_{28K} [1]. To our best knowledge these structures have never been reported in MR data. The aim of this work was to explore the anatomical structure of SN that is identifiable on MR images, to compare Perl's stained sections with MR susceptibility maps from the same sample and to identify *nigrosome*-like structures in high resolution post mortem and in vivo MR images.

Methods The MR scans were acquired on a 7T Philips Achieva scanner. In vivo data were collected on 4 healthy volunteers using an FFE sequence (20 slices, TR=484 ms, TE=14 ms, flip angle 40°, 0.34x0.34x1 mm³, in 11 min). The post mortem brain and brain stem of subjects with no known neurological conditions were obtained from the Queen's Medical Centre Nottingham, Neuropathology Department. They were fixed in 10% formalin, washed out in 0.09% saline for 24 hours before scanning and placed in a Perspex sphere filled with saline solution while being scanned. High resolution FFE scans of the whole brain (42 slices, TR=46 ms, TE=15 ms, flip angle 15°, 0.3x0.3x0.3 mm³ voxels, in 11.3 hours), and subsequently the resected brain stem (60 slices, TE=16 ms, TR=50 ms, flip angle 16°, 0.5x0.5x0.5 mm³ voxels, in 10.9 min) were acquired at 6 orientations to B₀ to allow a susceptibility map to be calculated. The susceptibility map was calculated from the resulting phase data using a k-space threshold method [2]. After scanning, the brain stem was sectioned and a Perl's stain was prepared on the chosen transverse slice. The resulting histology image was linearly registered with the MR 3D data and converted to grey scale. The susceptibility map and the Perl's stain of the brain stem were analysed using Matlab. Both images were divided into 300 identically-sized rectangles and down-sampled using the mean values calculated for the pixels inside the rectangles. The scatter plot in Figure 1 shows the transformed values from susceptibility and histology images. Three thresholds (60, 66 and 145) were applied to the susceptibility values dividing the SN image into three parts with different intensities. Itk-SNAP software was used for visual examination of the MR images of the whole brain in order to find the *nigrosome*-like structures in the SNpc, as well as their manual segmentation in the MR image of the post mortem brain.

Results The high resolution post mortem MR scan of the whole brain and in vivo scans showed dark patches which appeared to correspond to *nigrosomes* (Fig. 2). In the 3D visualisation, based on the manual segmentation, these regions appear like oval-shaped blobs and can be easily distinguished from blood vessels. They seem to be located in the transverse layers within the 3D volumetric data and do not agree with the simple layout identifying 5 different *nigrosomes* (Fig. 3) presented in [1]. Significant correlation was found between the Perl's stained histology image and the susceptibility map, confirmed by fitting a first degree polynomial (with coefficients: a₁=-0.08, a₀=203.46) to all of the points excluding background pixels marked in purple, as shown in Fig. 1. Three areas of the SN were discriminated by thresholding correspond to high, medium and low iron content. The characteristic *tear drop shaped* region marked in blue, which does not correspond to any anatomical structure, was also found in the in vivo data (Fig. 4). The

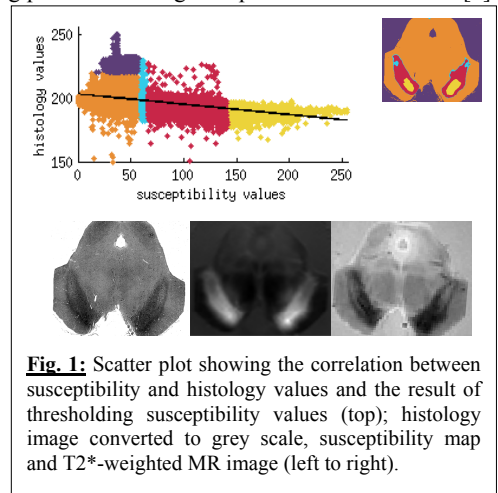


Fig. 1: Scatter plot showing the correlation between susceptibility and histology values and the result of thresholding susceptibility values (top); histology image converted to grey scale, susceptibility map and T2*-weighted MR image (left to right).

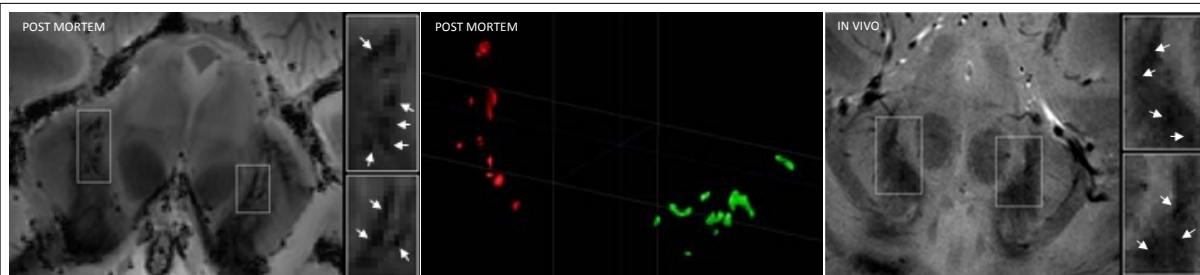


Fig. 2: *Nigrosome*-like structures are indicated by the white arrows in these transverse slices of post mortem (left) and in vivo (right) MR images; also shown is a 3D visualisation of the manually segmented structures in the post mortem MR image (centre).

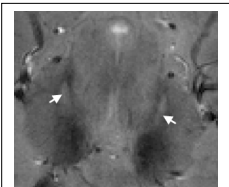


Fig. 4: The hypointense *tear drop shape* in the example MR in vivo image pointed to by arrows.

hypointensity visible in the T2* image might be a partial volume artefact, but could be also caused by the fluid content in this area. No medial-lateral variation in iron content consistent with the SNpc and SNpr definitions was found in the MR images.

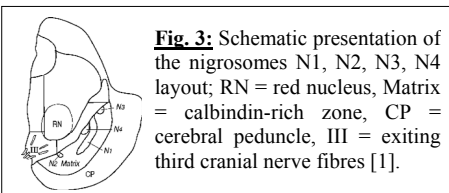


Fig. 3: Schematic presentation of the nigrosomes N1, N2, N3, N4 layout; RN = red nucleus, Matrix = calbindin-rich zone, CP = cerebral peduncle, III = exiting third cranial nerve fibres [1].

Conclusions High resolution MR images, both post mortem and in vivo, may allow identification of *nigrosome*-like structures in the SN pars compacta. Further validation is needed to confirm the presence of dopamine cells (tyrosinhydroxylase, TH staining) and level of calbindin D binding as nigrosomes are considered to be calbindin poor with fewer TH+ cells [1]. The susceptibility map correlates with the Perl's stain histology and can be used to identify the iron rich SN in MR data as well as allowing the examination of the levels of iron content in different parts of SN.

References [1] Damier et al., Brain, 1999, 122:1421-1436; [2] Wharton et al., MRM, 2010, 63:1292-1304.